JREE: Vol. 6, No. 4, (Autumn 2019) 41-48

Journal of Renewable Energy and Environment

Research Article

Journal Homepage: www.jree.ir

Numerical Investigation of Proton Exchange Membrane Fuel Cell Performance Enhancement by Geometrical Configuration Changing

Haleh Sadeghi[a], Iraj Mirzaei[a], Shahram Khalilaria[a], Sajad Rezazadeh[b*], Mojtaba Rasouli Gareveran[b]

[a] *Faculty of Mechanical Engineering, Urmia University, Urmia, Iran.*
[b] *Faculty of Mechanical Engineering, Urmia University of Technology, Urmia, Iran.*

PAPER INFO

Paper history:
Received 12 October 2019
Accepted in revised form 10 February 2020

Keywords:
Computational Fluid Dynamics
Fuel Cell,
Electrical Current Density
Membrane
Geometry

ABSTRACT

Among the renewable energy systems, fuel cells are of special significance about which more investigation is required. The principal goal of the present study is considering the effect of the geometry change on the fuel cell's performance. In this paper, a three-dimensional model of proton exchange membrane fuel cell has been numerically simulated with conventional cubic geometry. Afterwards, two brand-new cylindrical models have been proposed to compare and select the best model. The governing equations include mass, momentum, energy, species and electrical potential, which are discretized and solved using the method of computational fluid dynamics. The results obtained from numerical analyses were validated with those from experimental data, which showed acceptable agreement. For the above-mentioned models, changes in the species mass fraction, temperature, electric current density, and over-potential were analyzed in more detail. The results reveal that, in all three models, by decreasing the amount of cell voltage differences between the anode and the cathode, higher current density is produced, which leads to high input species consumption and, consequently, more water and heat generation. On the other hand, the four-channel cylindrical model is more efficient than the other two models and has shower pressure drop due to its shorter pathway. The results illustrated that, at V=0.6 **(V)**, the amount of the output current density in the four-channel model increased by approximately 18.4 %, compared to that in the other two models. Further, in this model, the material used in bipolar plates is less than that in the other models.

1. INTRODUCTION

Fuel cells are electrochemical devices that directly convert the chemical energy of reaction of a fuel and an oxidant (usually hydrogen and oxygen) into electricity. Shortly, fuel cells would be introduced as one of the main producers of energy. The researchers of PEM fuel cells claim many advantages for the system such as low noise, low operating temperature, fast start, simple building, and solid electrolyte. However, they need further research to be efficient, cheap to construct, and safe to operate [1-4]. A major drawback of PEM fuel cells, however, is that its production costs are still high, however, in recent years, attempts have been made to optimize the performance and reduce the outlay. In this technology, hydrogen and oxygen act respectively as fuel and oxidizing agent, producing power, water, and heat. By moving fuel in the anode channel and its collision with the catalyst layers, hydrogen protons (H^+) and electrons (e^-) are generated via oxidation action. Located in the heart of Proton Exchange Membrane Fuel Cell (PEMFC), a thin membrane is used as an electrolyte. Consequently, protons pass through the membrane and get to the cathode catalyst layer where they are combined with electrons and oxygen, producing water the heat. Membrane does not allow electrons to pass; therefore, an external collector is required through which the electrons can be transferred to the cathode side.

On the anode side, the semi-oxidation action is done and, on the opposite side, the reduction reaction is done. Porous surfaces facilitate species diffusion toward the electrochemical reaction area, thus reducing the amount of ohmic and concentration resistance. In the past, many attempts were made by researchers to develop the PEM fuel cells, especially efforts to increase the performance and reduce the costs [5]. Numerical modeling is one of the methods by which a basic understanding of the nature of the fuel cell can be achieved (see [6–14]) and the useful data can be extracted [15]. There are some factors that affect fuel cell performance, including pressure, temperature, incoming hydrogen, oxygen humidity, mass flow rate, and geometrical configuration. A review of previous works indicates that the degree of the influence of the geometrical shape of the fuel cell is more important than that of the other parameters that lead to considerable inefficiency of changes [16-19]. Rezazadeh et al. simulated a full three-dimensional PEMFC. In this research, some parameters such as oxygen consumption, water production, temperature distribution, ohmic losses, anode water activity, cathode over-potential, and fuel cell performance were investigated in more detail. The numerical simulations reveal that the important operating parameters are highly dependent on each other with respect to species distribution [20].

Ahmadi et al. studied PEMFC performance and mass transfer at various voltages [21]. Rezazadeh et al. studied the numerical investigation of the effect of the gas diffusion layer with semicircular prominences on polymer exchange membrane fuel cell performance and species distribution [22]. They concluded that an obstacle enhanced the cell performance.

On the other hand, they studied the effect of the obstacle on the gas diffusion layers, the velocity of the inlet gas distribution, and output current density [23]. Their numerical

*Corresponding Author's Email: sor.mems@gmail.com (S. Rezazadeh)

results showed that the prominence added to the GDL increased system performance. Ahmed et al. studied the results of the PEMFC survey by creating a new geometry and designing the deflected membrane electrode assembly [24].

Gobin Zhang and Koi Jiao studied a three-dimensional, two-phase model with wave-like channels. In this simulation, they found that by changing the flow field from parallel to spiral mode, the fuel cell performance would dramatically increase [25].

Yan Yin et al. simulated a three-dimensional, two-phase model with some baffles in its gas and oxygen channel to examine the effect of these baffles on the fuel cell performance.

They concluded that the mass transfer rate increased by applying the baffles [26]. Hosein Kalantari studied the effect of the porosity of the catalyst layers on the fuel cell performance and the distribution of water in the cell layers. The results of this study showed that with an increase in the cell voltage level, the water distribution level decreased on the cathode side [27].

In a numerical simulation, the effect of input gases, humidity, operating pressure, and working temperature on PEMFC was investigated by Zhuqing Zhang et al. They found that with increasing operating pressure, the amount of oxygen also increased, which has a good effect on the cell's fuel cell function [28]. Linhao Fan et al. investigated the optimization design of the cathode flow channel for proton exchange. In this research, two novel cathode channel designs (multi-plates structure channel and integrated structure channel) were proposed and investigated by a three-dimensional multiphase numerical model. The numerical results indicated that the PEMFC with 30° angle, 0.5 mm width, and 6.0 mm distance of air-guide plates exhibited the best performance, and the effect of plates angle on PEMFC performance was the most significant [29].

This article presents the results of a numerical investigation using a comprehensive three-dimensional, single-phase, non-isothermal and parallel flow model of a PEM fuel cell with straight channels. The governing equations are solved by a numerical method based on the finite volume method (FVM) and the obtained results are in good agreement with published data. The main goal of this work is to explain the mass transfer, temperature variation, and current density of the base model (model with straight flow channels) and two proposed models with a circular cross-section. It has been concluded that the new proposed models enjoy better efficiency than the base model with lower material for construction.

2. MATHEMATICAL MODELING

The base conventional model in this article is a straight cubic fuel cell, which is illustrated in Figure 1. The corresponding sections are as follows: anode gas channel, anode gas diffusion layer, anode catalyst layer, membrane, cathode catalyst layer, cathode gas diffusion layer, and cathode gas channel. The Membrane electrode assembly (MEA) consists of gas diffusion layers (GDL), catalyst layers (CTL), and membrane. Moreover, the geometrical and operational properties of the base are shown in the Table 1.

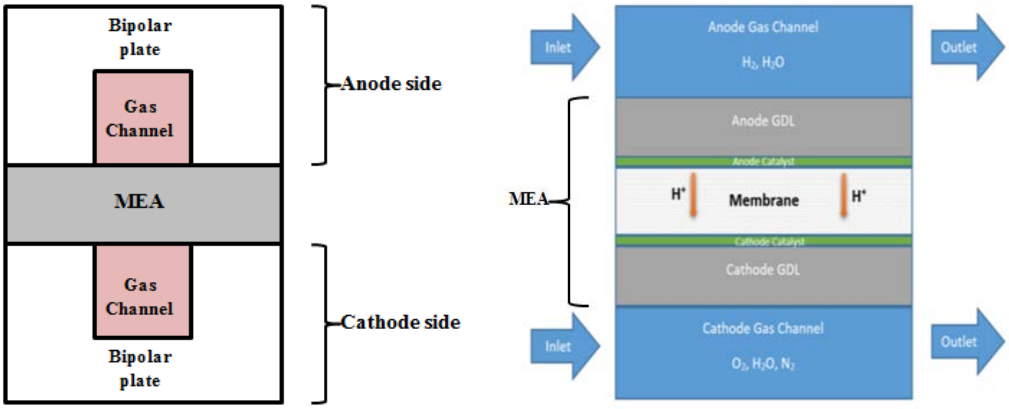

Figure 1. The base conventional model: front view (left) and beside view (right).

Table 1. The geometrical and operational properties of the base model.

Parameter	Symbol	Value	Unit
Channel length	L	0.05	m
Channel width	W	1e−3	m
Channel height	H	1e−3	m
Catalyst layer thickness	δ_{CL}	$0.0287e-3$	m
Gas diffusion layer thickness	δ_{GDL}	0.26e−3	m
Wet membrane thickness	δ_{mem}	0.23e−3	m
Faraday constant	F	96487	C/mol
Gas constant	R	8.314	kJ/K. mol
Anode pressure	P_a	3	atm
Cathode pressure	P_c	3	atm

Transfer coefficient, anode side	α_a	0.5	–
Transfer coefficient, anode side	α_c	1	–
Temperature	T	353.15	K
Fuel stoichiometric flow ratio	ξ_a	2	–
Electrode porosity	ε	0.4	–
Air stoichiometric flow ratio	ξ_c	2	–
Relative humidity of fuel and air	**Ψ**	**100**	%

2.1. Model assumptions

The following assumptions are used to solve the equations:

(1) Mixture of reactant gases is considered as the ideal gas.
(2) The fluid flow is incompressible and laminar (the Reynolds number is less than 200 and the Mach number is less than 0.3).
(3) The gas diffusion and catalyst layers are all homogenous materials.
(4) The fuel cell operates under steady state.

The water is in the vapor phase (the effect of liquid water is neglected).

2. 2. Governing equation

Different parts of the PEMFC have been modeled using the mass, momentum, species, electric charge and energy conservation equations. The mentioned equations and related boundary conditions with solution algorithm are presented in [29].

3. RESULTS AND DISCUSSION

In the present work, at first, the base cubic model has been simulated numerically and the corresponding results such as distribution of species, temperature and current density have been discussed in more detail. The comparison of the results of the proposed model and the reference data related to Wang et al. [30] can be seen in Figure 2, showing good conformity. Fig. 2 illustrates the polarization diagram of the fuel cell and represents the electrical current density versus cell voltage difference.

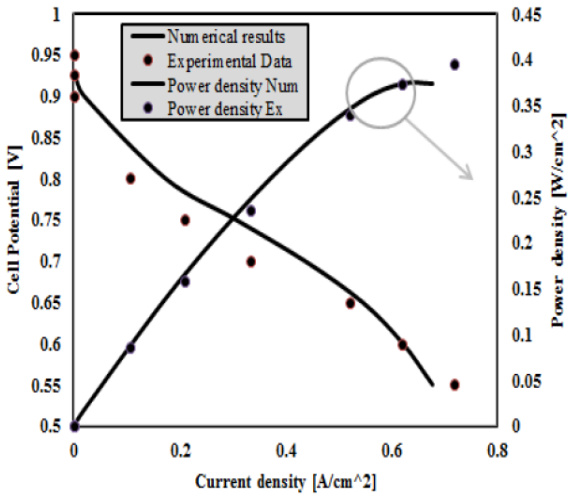

Figure 2. The Polarization curve for validation of numerical results with the results of Wang et al. [30].

3.1. Grid independency

In this three-dimensional model, to investigate the independence of the numerical solution from the number of computational cells, the model has been tested for various cells, and after testing its sensitivity, 240000 computational cells (meshes) have been selected. Figure 3 shows the mesh independency test.

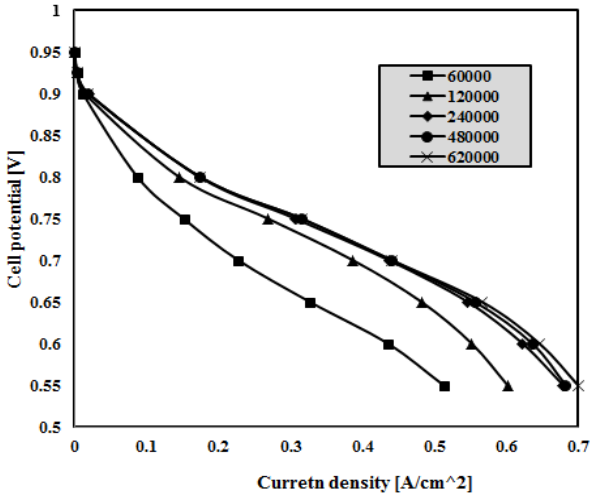

Figure 3. Grid independency test.

3.2. Oxygen distribution

In PEMFC, the amount of oxygen along the cathode is reduced due to its presence in the electrochemical reaction. Figure 4-a shows the mass fraction of oxygen in the lateral cross-sections at the cathode catalyst and the membrane interface. Figure 4-b illustrates the oxygen distribution at the interface of gas diffusion and catalyst layers.

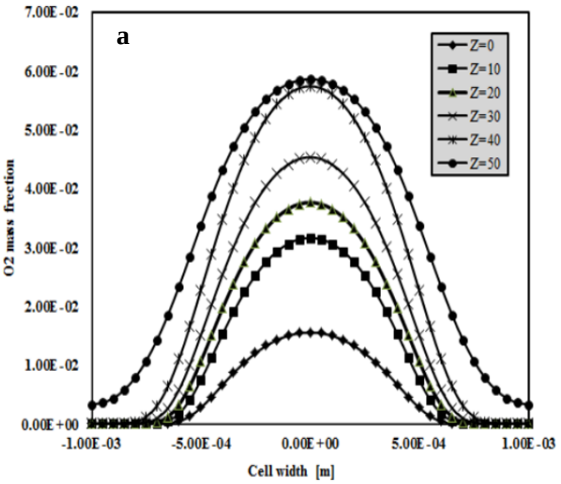

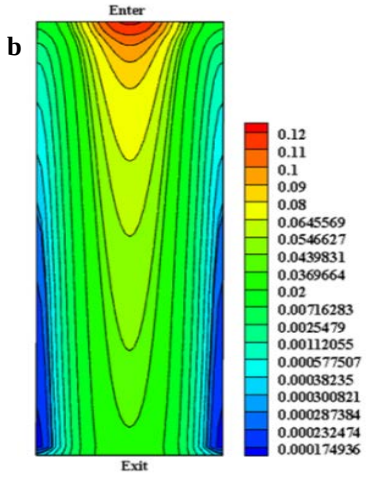

Figure 4. Longitudinal mass fraction of (a) oxygen and (b) transverse mass fraction of oxygen at V=0.6 (V).

3.3. Water distribution

As shown in Figures 5, the amount of water increases along the cell due to its production in reaction and also its penetration from the anode side to the cathode side.

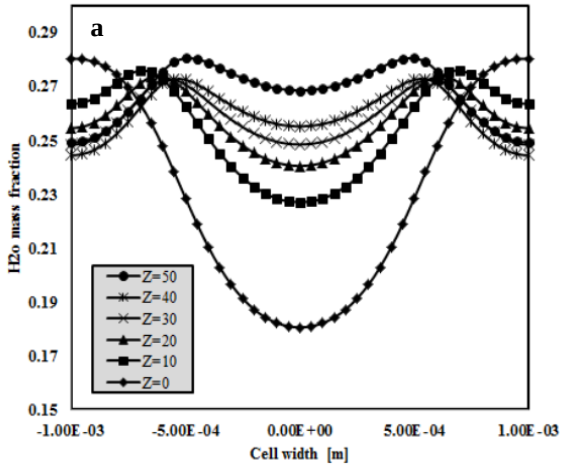

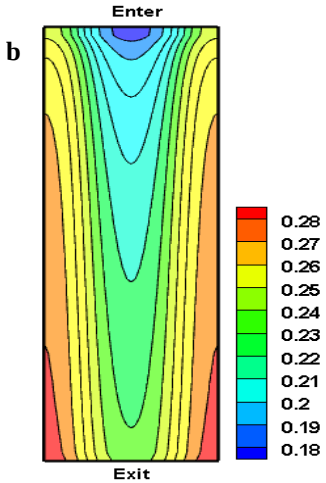

Figure 5. (a) Transverse mass fraction of water and (b) longitudinal mass fraction of water at V= 0.6(V) on the cathode side.

Figure 6 shows the distribution of water for different cross-sections of the fuel cell at V=0.6 (V). As the shown in the figure, the water gradually decreases on the anode side which results from the migration of water particles to the cathode side. Consequently, the water magnitude increases along the cell on the cathode side offer of the mentioned reasons.

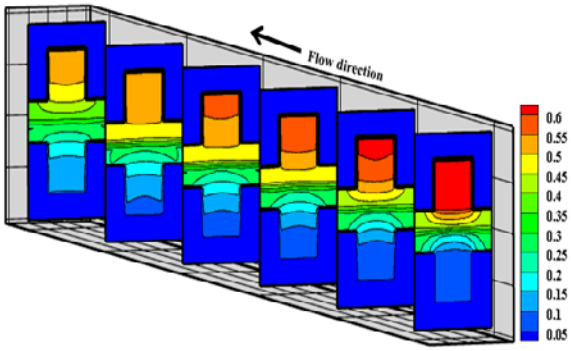

Figure 6. Mass distribution of water in total fuel cell for V=0.6 (V).

4. PROPOSED MODELS

The new proposed models presented in this paper include two cylindrical models represented in Figures 7 and 8. The mentioned figures are the cross-section side view of the cells. In these three-dimensional models, approximately 243,000 computational cells have been generated, which are almost similar to those in the base model. To make a correct comparison between the base model and proposed models, the surface area of the reaction, the area of inlet gas channels, the mass flow rate of the inlet flow and their temperatures are assumed to be the same.

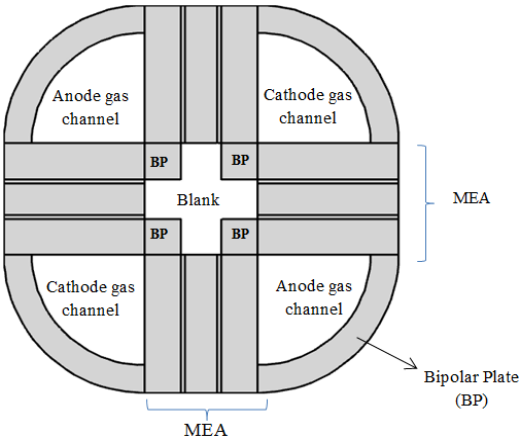

Figure 7. Front view of the four-channel model.

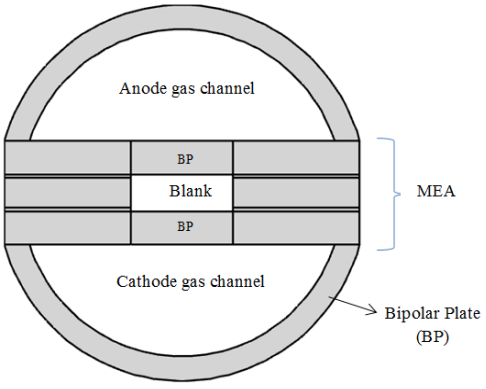

Figure 8. Front view of the two-channel model.

In the models mentioned above, the surface area of the reaction is equal to the surface area of the reaction of the base model. Therefore, the length of the four-channel model is half than of the other models. In Table 2, the geometric dimensions of the proposed model are presented.

Table 2. The geometrical and operational properties of the proposed models.

Parameter	2 channel	4 channel	Unit
Channel length	0.05	0.025	m
Channel width	0.0008	0.0008	m
Channel height	1e−3	1e−3	m
Catalyst layer thickness	0.028*e*−3	0.028*e*−3	m
Gas diffusion layer thicknes	0.26e−3	0.26e−3	m
Wet membrane thickness	**0.23e−3**	**0.23e−3**	**m**

Figure 9 shows the current density comparison between the three models at V=0.6 (V) and V=0.4(V). The result shows that, in the four-channel model, despite a reduction in bipolar plates volume compared to the base model, due to the dual connection between anode and cathode sides and, consequently, the better distribution of reactants in the reaction area, a better performance is shown.

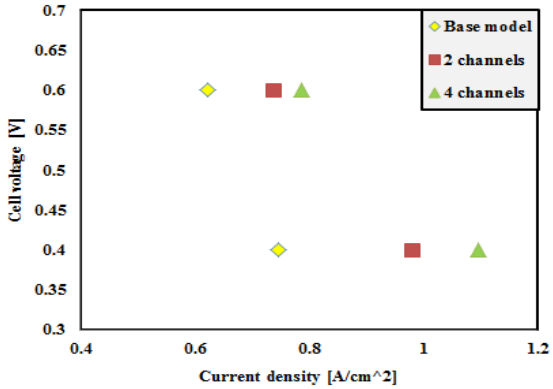

Figure 9. Comparison of the produced electric current density for the models presented at V=0.6(V) and V= 0.4(V).

As shown in Figure 10, oxygen is consumed from the beginning to the end of the cell, due to its participation in the electrochemical reaction. At high voltages, where a low current density is generated, the oxygen consumption is greatly reduced, however, at low cell voltages, high current density is generated and the amount of oxygen approaches near to zero, which indicating the oxygen consumption. Among the models presented, the four-channel model has higher oxygen consumption than the other models due to its higher reaction level; thereforethe, the mass fraction of oxygen is lower.

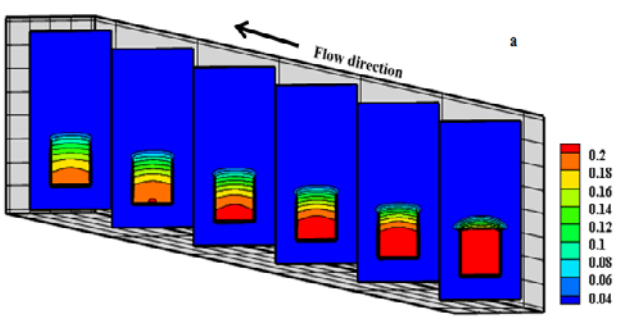

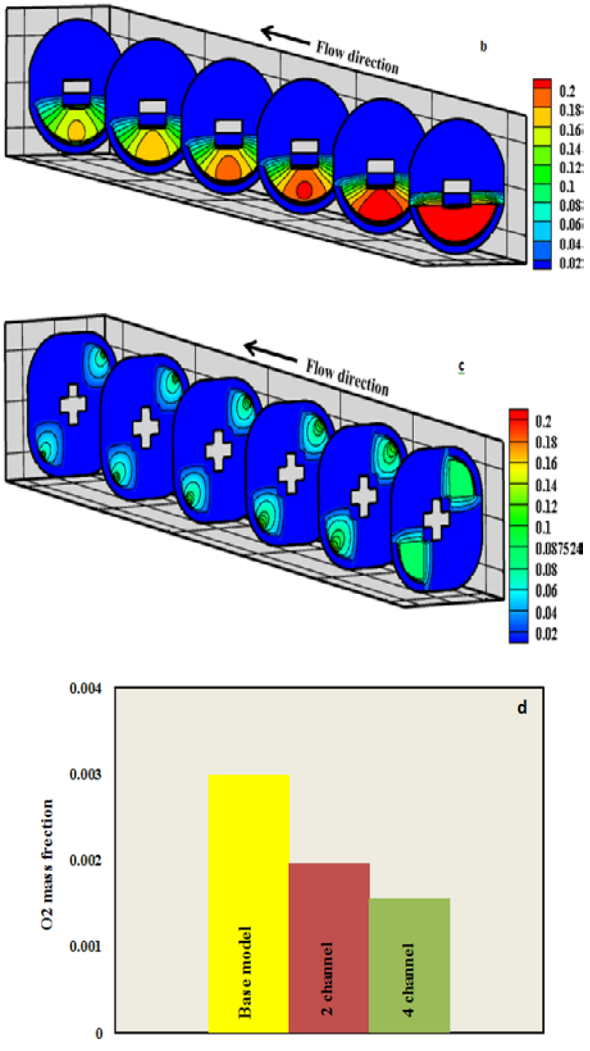

Figure 10. Distribution of oxygen mass fraction: base models (a), two-channels (b) and four-channels (c) and the average of oxygen mass fraction at the membrane and cathode catalyst layer at V=0.4 (V).

Due to the migration of water molecules from the anode side to the cathode for transferring the H+, the water mass fraction along the cell decreases on the anode side. Further, on the cathode side, due to the electrochemical reactions and water production process, the number of the mentioned species is higher. Therefore, it can be concluded that the water magnitude at anode side decreases and on the cathode side increases along the cell. Therefore, as shown in Figure 11, the production of water in the four-channel model is higher than that in other models because of its higher performance, and consequently, faster reaction rate. As is clear, the average water magnitude in the model with four channels is more than that in the other ones.

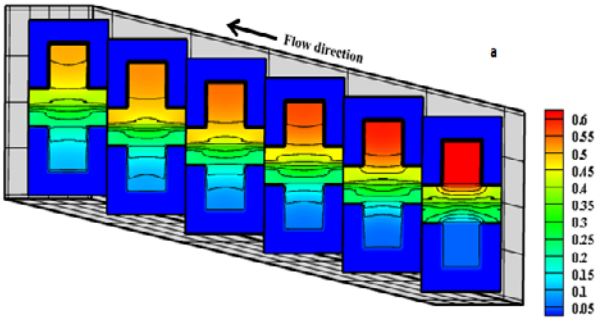

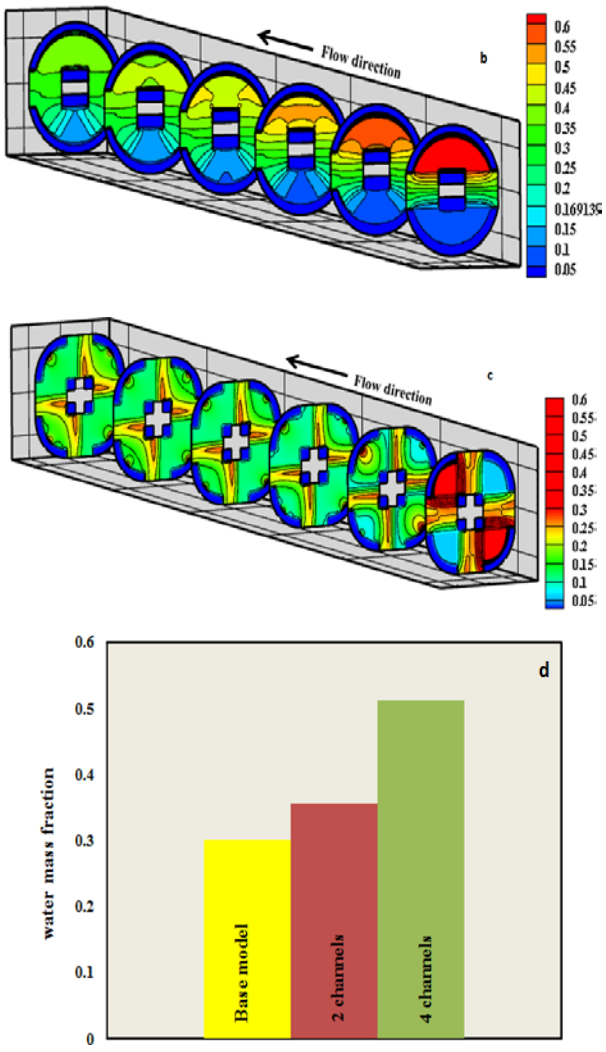

Figure 11. Distribution of water mass fraction: base models (a), two channels (b) and four channels (c) and the average of water mass fraction at the membrane and cathode catalyst layer at V=0.4 (V).

According to Figure 12, the maximum temperature of the fuel cell is in the entrance region of the cell, but due to the production of water because of electrochemical reaction and cooling effects by the produced water, the exit region of the cell experiences a temperature drop. The heat generated in the fuel cell relates to the electrochemical reaction rate, and it is clear that while the new model with four channels produces higher current density than the other models, its temperature distribution is higher too. The average temperature in the model with four channels illustrates the higher magnitude.

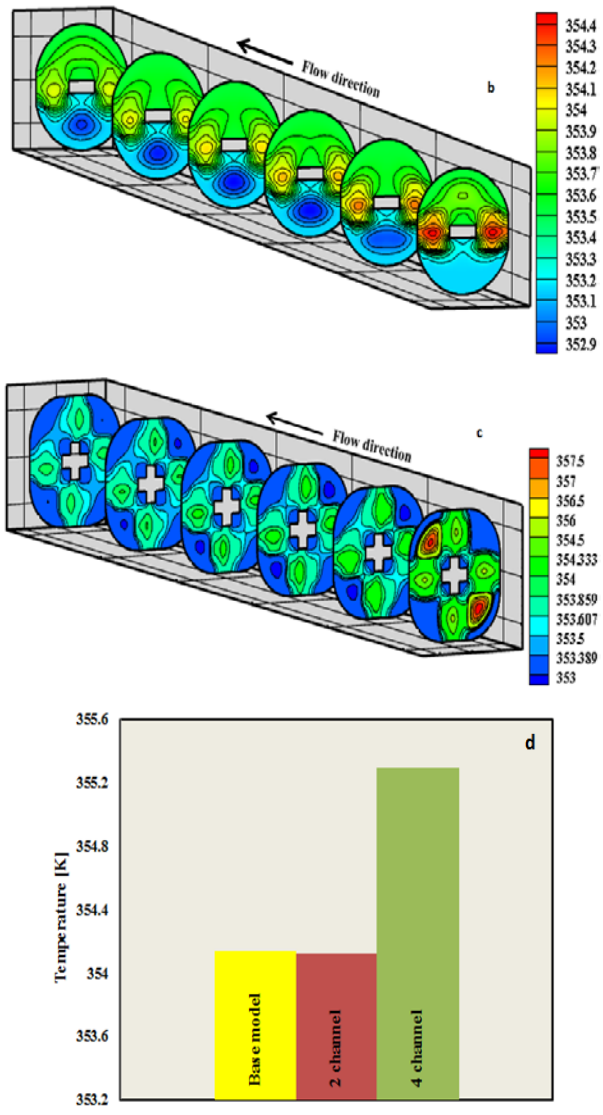

Figure 12. Distribution of temperature: base models (a), two channels(b) and four channels (c) and the average of temperature at the membrane and cathode catalyst layer at V=0.4 (V).

As shown in Figure 13, the current density along the fuel cell decreases regularly because the moisture content of the membrane reduces and, consequently, the protonic conductivity of the membrane diminishes; therefore, the current density decreases. The current densities depend on the electrochemical reaction rate, and while its amount in the proposed four-channel model is high, the mentioned model indicates better performance.

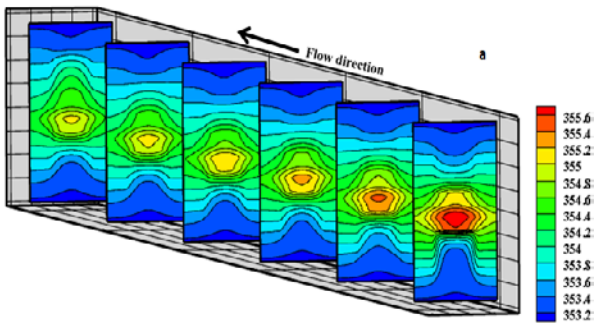

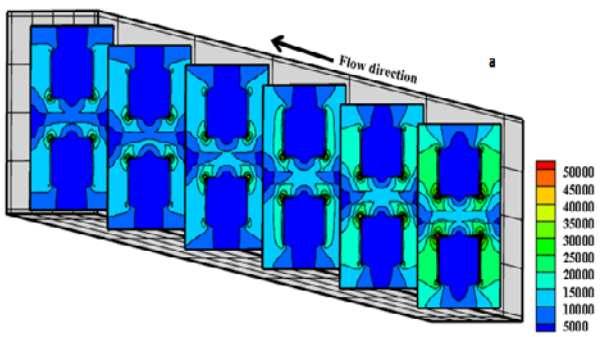

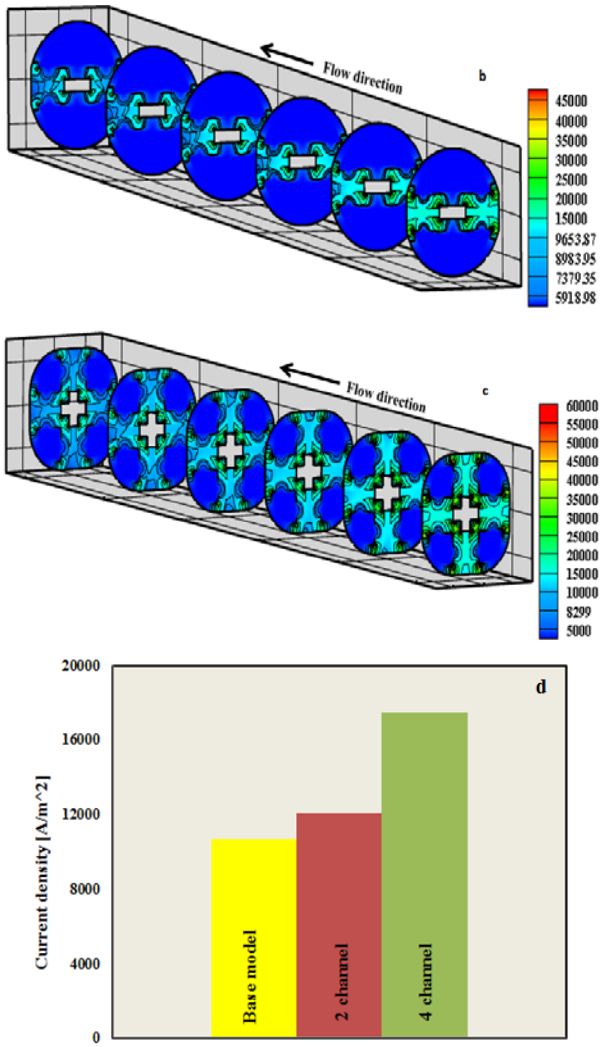

Figure 13. Distribution of current density: base models (a), two channels (b) and four channels (c) and the average of current density at the membrane and cathode catalyst layer at V=0.4 (V).

Figure 14 shows the pressure drop for models at different cell voltages. While the four-channel model is shorter and does not have a sharp corner, it has lower pressure drop than the other models. Further, the figure indicates that the pressure drop is the same for all cell voltages. It is implied that the pressure decline does not depend on the cell voltage. The base models because of their longer length and sharp corners have a greater pressure decline.

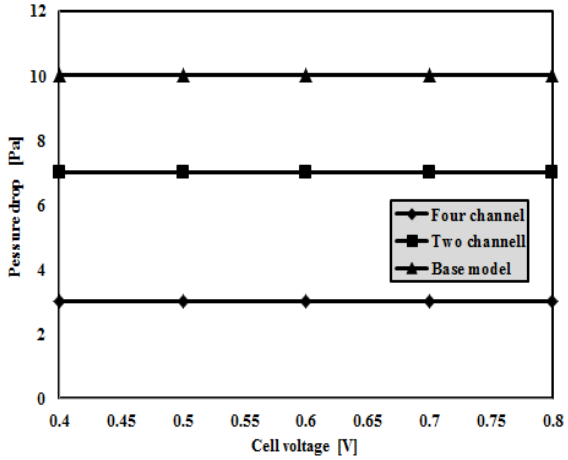

Figure 14. Pressure drop at different cell voltages.

5. CONCLUSIONS

In this paper, three types of polymer fuel cells were simulated in cubic and cylindrical forms numerically. The base model results (conventional cubic model) were validated with popular published data, and the new cylindrical models were compared with the base model and the obtained numerical results were presented in more detail. For solving the governing equations, the finite volume method was used. Generally, the summarized results are presented below.

In all three models, the boundary conditions are the same, but for keeping the reaction area constant, the lengths of models were different. The newly proposed models with cylindrical cross-sections, especially the four-channel model, can produce higher current density the than cubic model. Thus, it can be concluded that the mentioned model has higher performance. The oxygen mass fraction along the fuel cell for all three models at V=0.4 (V) was investigated, and the results showed that the oxygen consumption in the four-channel model was higher than that in the other models due to higher electricity generation; therefore, the water produced in the mentioned model was higher than that in the other ones. On the other hand, the pressure drop of models was studied, and the results illustrated that the four-channel model had lower pressure decline than the others because it has a short length and does not have any sharp corners. Finally, the user can choose the mentioned model for any possible application.

6. ACKNOWLEDGEMENT

We gratefully acknowledge Urmia University of Technology computer center manager for allowing us to use their computers.

NOMENCLATURE

a	Water activity
C	Molar concentration (mol m^{-3})
D	Mass diffusion coefficient (m^2 s^{-1})
F	Faraday constant (C mol^{-1})
I	Local current density (A m^{-2})
J	Exchange current density (A m^{-2})
K	Permeability (m^2)
M	Molecular mass (kg mol^{-1})
n_d	Electro-osmotic drag coefficient
P	Pressure (Pa)
R	Universal gas constant (J mol^{-1} K^{-1})
T	Temperature (K)
T	Thickness
u	Velocity vector
V_{cel}	Cell voltage
V_{oc}	Open-circuit voltage
W	Width
X	Mole fraction
α	Water transfer coefficient
ε^{eff}	Effective porosity
ρ	Density (kg m^{-3})
Φ_e	Electrolyte phase potential
μ	Viscosity (kg $m^{-1}s^{-1}$)
σ_m	Membrane conductivity ($1.ohm^{-1}m^{-1}$)
λ	Water content in the membrane
ζ	Stoichiometric ratio
η	Over-potential (v)
λ_{eff}	Effective thermal conductivity (w $m^{-1}k^{-1}$)
a	Anode
c	Cathode
ch	Channel
k	Chemical species

m	Membrane
MEA	Membrane electrolyte assembly
ref	Reference value
sat	Saturated
w	Water

REFERENCES

1. Sadiq Al-Baghdadi, M.A.R. and Shahad Al-Janabi, H.A.K., "Modeling optimizes PEM fuel cell performance using three-dimensional multi-phase computational fluid dynamics model", ***Energy Conversion and Management***, Vol. 48, No. 12, (2007), 3102-3119. (https://doi.org/10.1016/j.enconman.2007.05.007).
2. Kilic, M.S., Korkut, S. and Hazer, B., "Electrical energy generation from a novel polypropylene grafted polyethylene glycol based enzymatic fuel cell", ***Analytical Letters***, Vol. 47, No. 6, (2014), 983-995. (https://doi.org/10.1080/00032719.2013.860536).
3. Karthikeyan, R., Uskaikar, H.P. and Berchmans, S., "Electrochemically prepared manganese oxide as a cathode material for a microbial fuel cell", ***Analytical Letters***, Vol. 45, No. 12, (2012), 1645-1657. (https://doi.org/10.1080/00032719.2012.677786).
4. Saheb, A.H. and Seo, S.S., "Polyaniline /Au electrodes for direct methanol fuel cells", ***Analytical Letters***, Vol. 44, No. 12, (2011), 2221-2228. (https://doi.org/10.1080/00032719.2010.546031).
5. Grujicic, M. and Chittajallu, K.M., "Design and optimization of polymer electrolyte membrane (PEM) fuel cells", ***Applied Surface Science***, Vol. 227, (2004), 56-72. (https://doi.org/10.1016/j.apsusc.2003.10.035).
6. Xing, X.Q., Lum, K.W., Poh, H.J. and Wu, Y.L., "Optimization of assembly clamping pressure on performance of proton-exchange membrane fuel cells", ***Journal of Power Sources***, Vol. 195, No. 1, (2010), 62-68. (https://doi.org/10.1016/j.jpowsour.2009.06.107).
7. Chang, W.R., Hwang, J.-J., Weng, F.-B. and Chan, S.-H., "Effect of clamping pressure on the performance on a PEM fuel cell", ***Journal of Power Sources***, Vol. 166, (2007), 149-154. (https://doi.org/10.1016/j.jpowsour.2007.01.015).
8. Lange, K.J., Sui, P.-C. and Djilali, N., "Determination of effective transport properties in a PEMFC catalyst layer using different reconstruction algorithms", ***Journal of Power Sources***, Vol. 208, (2012), 354-365. (https://doi.org/10.1016/j.jpowsour.2011.11.001).
9. Amphlett, J.C., Baumert, R.M., Mann, R.F., Peppley, B.A., Roberge, P.R. and Harris, T.J., "Performance modeling of the Ballard Mark IV solid polymer electrolyte fuel cell. I. Mechanistic model development", ***Journal of the Electrochemical Society***, Vol. 142, No. 1, (1995), 9-15. (10.1149/1.2043866J. Electrochem. Soc. 1995 volume 142, issue 1, 1-8).
10. He, G., Yamazaki, Y. and Abudula, A., "A three-dimensional analysis of the effect of anisotropic gas diffusion layer (GDL) thermal conductivity on the heat transfer and two-phase behavior in a proton exchange membrane fuel cell (PEMFC)", ***Journal of Power Sources***, Vol. 195, (2010), 1551-1560. (https://doi.org/10.1016/j.jpowsour.2009.09.059).
11. Oetjen, H.-F., Schmidt, V.M., Stimming, U. and Trila, F., "Performance data of a proton exchange membrane fuel cell using H_2/Co as fuel gas", ***Journal of the Electrochemical Society***, Vol. 143, No. 12, (1996), 3838-3842. (10.1149/1.1837305J. Electrochem. Soc. 1996 volume 143, issue 12, 3838-3842).
12. Büchi, F.N. and Srinivasan, D., "Operating proton exchange membrane fuel cells without external humidification of the reactant gases", ***Journal of the Electrochemical Society***, Vol. 144, No. 8, (1997), 2767-2772. (10.1149/1.1837893J. Electrochem. Soc. 1997 volume 144, issue 8, 2767-2772).
13. Uribe, F.A., Gottesfeld, S. and Zawodzinski, T.A., "Effect of ammonia aspotential fuel impurity on proton exchange membrane fuel cell performance", ***Journal of the Electrochemical Society***, Vol. 149, No. 3, (2002), A293-A296. (10.1149/1.1447221J. Electrochem. Soc. 2002 volume 149, issue 3, A293-A296).
14. Ticianelli, E.A., Derouin, C.R. and Srinivasan, S., "Localization of platinumin low catalyst loading electrodes to attain high power densities in SPEfuel cells", ***Journal of Electroan Alytical Chemistry and Interfacial Lectrochemistry***, Vol. 251, (1988), 275–295. (https://doi.org/10.1016/0022-0728) (88)85190-8).
15. Yao, K.Z., Karan, K., McAuley, K.B., Oosthuizen, P., Peppley, B. and Xie, T., "A review of mathematical models for hydrogen and direct methanol polymer electrolyte membrane fuel cells", ***Fuel Cells***, Vol. 4, No. 1-2, (2004), 3-29. (https://doi.org/10.1002/fuce.200300004).
16. Natarajan, D. and Nguyen, T.V., "A two-dimensional, two-phase, multi component, transient model for the cathode of a proton exchange membrane fuel cell using conventional gas distributors", ***Journal of the Electrochemical Society***, Vol. 148, No. 12, (2001), A1324-A1335. (10.1149/1.1415032J. Electrochem. Soc. 2001 volume 148, issue 12, A1324-A1335).
17. Ahmadi, N., Rezazadeh, S., Yekani, M., Fakouri, A. and Mirzaee, I., "Numerical investigation of the effect of inlet gases humidity on polymer exchange membrane fuel cell (PEMFC) performance", ***Transactions of the Canadian Society for Mechanical Engineering***, Vol. 37, (2013), 1-20. (https://doi.org/10.1139/tcsme-2013-0001).
18. Lum, K.W. and McGuirk, J.J., "Three-dimensional model of a complete polymer electrolyte membrane fuel cell – model formulation, validation and parametric studies", ***Journal of Power Sources***, Vol. 143, (2005), 103-124. (https://doi.org/10.1016/j.jpowsour.2004.11.032).
19. Ahmed, D.H. and Sung, H.J., "Effects of channel geometrical configuration and shoulder width on PEMFC performance at high current density", ***Journal of Power Sources***, Vol. 162, (2006), 327-339. (https://doi.org/10.1016/j.jpowsour.2006.06.083).
20. Rezazadeh, S., Mirzaee, I., Pourmahmoud, N. and Ahmadi, N., "Three-dimensional computational fluid dynamics analysis of a proton exchange membrane fuel cell", ***Journal of Renewable Energy and Environment***, Vol. 1, No. 1, (2015), 30-42.
21. Pashaee Golmarz, T., Rezazadeh, S. and Bagherzadeh, N.,"Numerical study of curved-shape channel effect on performance and distribution of species in a proton-exchange membrane fuel cell: Novel structure", ***Journal of Renewable Energy and Environment* (JREE)**, Vol. 5, No. 2, (2018), 10-21.
22. Ahmadi, N., Pourmahmoud, N., Mirzaee, I. and Rezazadeh, S.,"Three-dimensional computational fluid dynamic study of effect of different channel and shoulder geometries on cell performance", ***Australian Journal of Basic and Applied Sciences***, Vol. 5, No. 12, (2011), 541-556.
23. Ahmadi, N., Rezazadeh, S., Mirzaee, I. and Pourmahmoud, N., "Three-dimensional computational fluid dynamic analysis of the conventional PEM fuel cell and investigation of prominent gas diffusion layers effect", ***Journal of Mechanical Science and Technology***, Vol. 26, No. 8, (2012), 1-11. (https://doi.org/10.1007/s12206-012-0606-1).
24. Ahmed, D.H. and Sung, H.J., "Design of a deflected membrane electrode assembly for PEMFCs", ***International Journal of Heat and Mass Transfer***, Vol. 51, (2008), 5443-5453. (https://doi.org/10.1016/j.ijheatmasstransfer.2007.08.037).
25. Zhang, G. and Jiao, K.," Three-dimensional multi-phase simulation of PEMFC at high current density utilizing Eulerian-Eulerian model and two-fluid model", ***Energy Conversion and Management***, Vol. 176, (2018), 409-421. (https://doi.org/10.1016/j.enconman.2018.09.031).
26. Yin, Y., Wang, X., Shangguan, X., Zhang, J. and Qin, Y., "Numerical investigation on the characteristics of mass transport and performance of PEMFC with baffle plates installed in the flow channel", ***International Journal of Hydrogen Energy***, Vol. 43, No. 16, (2018), 8048-8062. (https://doi.org/10.1016/j.ijhydene.2018.03.037).
27. Kalantari, H., "Numerical analysis of water distribution in various layers of proton exchange membrane fuel cells", ***Computers and Chemical Engineering***, Vol. 118, (2018), 14-24. (https://doi.org/10.1016/j.compchemeng.2018.07.004).
28. Zhang, Z., Liu, W. and Wang, Y., "Three dimensional two-phase and non-isothermal numerical simulation of multi-channels PEMFC", ***International Journal of Hydrogen Energy***, Vol. 44, No. 1, (2018), 379-388. (https://doi.org/10.1016/j.ijhydene.2018.05.149).
29. Fan, L., Niu, Z., Zhang, G. and Jiao, K., "Optimization design of the cathode flow channel for proton exchange membrane fuel cells", ***Journal of Energy Conversion and Management***, Vol. 171, (2018), 1813-1821. (https://doi.org/10.1016/j.enconman.2018.06.111).
30. Wang, L., Husar, A., Zhou, T. and Liu, H., "A parameteric study of PEM fuel cell performances", ***International Journal of Hydrogen Energy***, Vol. 28, (2003), 1263-1272. (https://doi.org/10.1016/S0360-3199 (02)00284-7).
31. Meredith, R.E. and Tobias, C.W., Advances in electrochemistry and electrochemical engineering", Tobias, C.W. ed., Interscience Publishers, New York, (1960).